

Universal stabilizing mechanism for transition-metal polytetrahedrally packed phases

Rob Phillips* and A. E. Carlsson

Department of Physics, Washington University in Saint Louis, Campus Box 1105, Saint Louis, Missouri 63130-4899

(Received 27 November 1989; revised manuscript received 30 April 1990)

We describe the electronic factors leading to structural stability in the class of transition-metal alloys exhibiting polytetrahedral packing (PTP). In a cluster expansion for the total energy, the lowest-order terms which obtain the correct chemical trends correspond to angular forces. These contain an energetic penalty for four-body clusters with 90° angles. Such clusters are uniformly absent in the PTP phases. The four-body contribution is roughly structure independent within the PTP class.

I. INTRODUCTION

Polytetrahedrally packed (PTP) structures are those which are built entirely out of tetrahedral packing units.¹ In contrast, the fcc structure consists of both tetrahedral and octahedral units, while the bcc structure is an intermediate case with the octahedra containing second-neighbor bonds. The tetrahedral packing leads to characteristic polyhedra, which are labeled Z12, Z14, Z15, and Z16, where the numbers refer to the coordination number of the atom centering the polyhedron. PTP structures are almost always found in alloys and compounds rather than elemental systems. The simplest example of a PTP structure is the *A*15 structure, which has eight atoms per unit cell. Two of these are surrounded by Z12 polyhedra, which are icosahedra, and the remaining six by Z14 polyhedra. The remaining PTP phases, such as the well-known σ phase, contain much larger unit cells. Inspection of phase diagrams for binary transition-metal compounds reveals that the PTP phases occur over a wide range of both composition and temperature. Any satisfactory theory of alloy phase stability must explain the presence of these structures in the phase diagram.

PTP structures are of fundamental interest because they are a precisely characterized packing of structural units which are believed to be present in aperiodic systems. For example, it has been proposed that both liquids and metallic glasses have a large degree of local tetrahedral order.² Some types of icosahedral phases are believed to share structural motifs with PTP phases, and, in fact, to be very closely related in structure.³ Recent work on the Ti-Mn quasicrystal⁴ has demonstrated the presence of nearly identical structural motifs in the quasicrystal and its crystalline transformation products. In particular, it is now believed⁴ that both structures contain icosahedral building blocks. This work strengthens the evidence for a connection between the PTP phases and icosahedral quasicrystals, since the PTP phases always exhibit partial local icosahedral order. Because the atomic positions in the periodic PTP phases are precisely established in many cases, it is possible to investigate the local bonding energetics without having to make arbi-

trary assumptions about these positions. In addition, as mentioned above, the PTP phases are of practical interest because of their frequent appearance as undesirable brittle "interloper" phases⁵ in transition-metal alloy phase diagrams.

Our aim is to identify the lowest-order *r*-space interactions which stabilize the transition-metal PTP phases as a class. Because of the similar short-range order in these phases, we expect certain terms in our cluster expansion for the total energy to be insensitive to the differences from one PTP structure to the next, thus establishing unifying energetic factors which stabilize them. The treatment of the PTP phases as a class, rather than on a case-by-case basis, is motivated by previous empirical work by Watson and Bennett,⁶ which has identified the stability of the class of PTP structures with a characteristic range of "effective *d*-hole counts" and limits on atomic-size ratios. They conclude that the average filling of the *d* band is crucial in establishing which alloys will form PTP phases, while for the non-Laves PTP phases, the atomic-size ratios are a less important factor. Previous theoretical work on a few specific PTP structures,⁷⁻⁹ as well as the empirical work, suggest that electronic effects are as important, if not more so, than the atomic-size effects (at least for the non-Laves phases). This is particularly evident in the *A*15 "size-reversal" compounds,⁶ such as V_3Rh , in which the smaller (larger) atoms occupy sites normally filled by the larger (smaller) atoms. Turchi, Treglia, and Ducastelle have performed detailed analyses^{7,8} of the stability of *A*15- and Laves-phase compounds, supporting the claim that the *d*-band filling is crucial in determining the stability of PTP compounds.

In this work we use recently developed transition-metal interatomic potentials to examine PTP structural stability. These potentials have a functional form derived from the moments of the electronic density of states using a tight-binding Hamiltonian. We show that the dominant electronic effects can be described by a four-body interaction which penalizes squares of nearest-neighbor atoms, and favors tetrahedral configurations. In all of the PTP structures which we treat, this interaction provides a large stabilizing contribution, which typically exceeds the magnitude of the atomic-size effects. We are not, howev-

er, able to discriminate reliably between different PTP phases. In fact, all of the PTP structures which we consider have essentially the same four-body energy.

The remainder of the paper is organized as follows. In Sec. II we describe the derivation of the potentials from our treatment of the total energy. In Sec. III we present our results for the six PTP structures that we have considered. We emphasize the direct connection between the energy and the geometry, and the energetic invariants which are found in the four-body terms. Section IV concludes with a discussion of the relevance of our results to aperiodic systems.

II. METHODOLOGY

Our picture of the stability of the PTP phases is based on effective interatomic potentials obtained from a moment analysis of a d -electron nearest-neighbor tight-binding Hamiltonian H .^{10,11} The Hamiltonian is given by

$$H = \sum_i \sum_\alpha \varepsilon_i |i, \alpha\rangle \langle i, \alpha| + \sum_{ij} \sum_{\alpha, \beta} h_{ij}^{\alpha\beta} |i, \alpha\rangle \langle j, \beta|, \quad (1)$$

where i (j) are site indices, α (β) label the orbitals, ε_i is the diagonal site energy, and the $h_{ij}^{\alpha\beta}$ are coupling matrix elements, as determined by Slater-Koster theory. The moments of the electronic density of states, which are determined by the local atomic environment, are defined by $\mu_n = \text{Tr}(H^n)$ and can be written¹⁰ as sums of n -body path terms involving the interatomic couplings $h_{ij}^{\alpha\beta}$ in the tight-binding Hamiltonian. For example, the second moment

$$\mu_2 = \sum_{i, j, \alpha, \beta} h_{ij}^{\alpha\beta} h_{ji}^{\beta\alpha}$$

is given as a sum of radial pair contributions. The higher-order moments ($n \geq 3$) are angle-dependent functions as long as the orbitals in the tight-binding basis have angular momentum character $l \geq 1$. This angle dependence is responsible for the stability of the PTP structures.

Given the moments, the total energy is calculated using

$$E_{\text{tot}} = \frac{1}{2} \sum_{ij} \phi_{\text{rep}}(\mathbf{r}_i, \mathbf{r}_j) + 2 \int_{-\infty}^{\varepsilon_F} dE \rho(E) E, \quad (2)$$

where ϕ_{rep} is a repulsive pair potential and $\rho(E)$ is the electronic density of states (DOS). The factor of 2 preceding the integral accounts for spin degeneracy. The DOS is determined using the maximum-entropy method,¹² and is given by

$$\rho(E) = \exp \left[- \sum_{n=0}^N \lambda_n E^n \right], \quad (3)$$

where the λ_n are Lagrange multipliers which are nonlinear functions of the moments. Given the total energy as expressed in Eq. (2), the calculation of the effective interatomic potentials proceeds directly.

The effective potential associated with an n -body cluster is given by¹³

$$V_n^{\text{eff}}(\mathbf{r}_1, \dots, \mathbf{r}_n) = \sum_{m=n}^N \frac{\partial E}{\partial \mu_m} \mu_m^{ij \dots n}(\mathbf{r}_1, \dots, \mathbf{r}_n), \quad (4)$$

where $\mu_m^{ij \dots n}(\mathbf{r}_1, \dots, \mathbf{r}_n)$ is the contribution of the direct n -body path to the m th moment, and E is an approximation to the electronic band energy obtained from the density of states (3). Equation (4) defines a linearization of the dependence of E on the μ_n , which simplifies the visualization of the energetics. The angular dependence of the potentials comes directly from that of the associated moments. In the cases we have considered, the linearization gives errors of less than 10% in structural energy differences. The pair energy is supplemented by a purely repulsive term which prohibits unphysically close approaches and includes atomic-size effects. This repulsive term is computed by fitting to the elemental equilibrium lattice constants and bulk moduli on the fcc lattice, obtained by self-consistent band-structure calculations.¹⁴ The form of the repulsive term we have used is given by

$$\phi_{\text{rep}}(\mathbf{r}_i, \mathbf{r}_j) = A e^{-\lambda(r_{ij} - r_0)}. \quad (5)$$

For ease of interpretability, the electronic band energy is calculated within the common-band approximation,⁹ in which single-site energy differences are ignored, and the matrix elements coupling different sites are assumed to be independent of the chemical identity of the constituents. We have found that including corrections to this approximation results in only minor effects, mainly a 10% shift in the region of d -electron counts for which the PTP phases are preferred. We have used seven different types of tight-binding parametrizations.¹⁵ The decay schemes and ratios of tight-binding parameters that have been used are shown in Table I. We find that the dominant four-body term mentioned above is only slightly affected by the choice of tight-binding parameters. The contribution of this term to the PTP-fcc energy difference, averaged over the PTP structures that are treated, ranges from -0.16 to -0.20 eV for various parametrizations. The chemical trends in the calculated structural-energy

TABLE I. Parameter sets examined for common-band PTP-fcc structural-energy differences. The units for scheme (a) are in units of $\text{eV} \text{ \AA}^5$, those in scheme (b) are in units of $\text{eV} \text{ \AA}^\alpha$, and those in schemes (c)–(f) are in units of eV. For further discussion of tight-binding couplings, see W. A. Harrison, *Electronic Structure and the Properties of Solids* (Freeman, San Francisco, 1980).

Decay scheme	σ	π	δ
(a) r^{-5}	-90.034	38.509	-3.525
(b) $(r_0 - r)^\alpha$	-0.876	0.375	-0.034
(c) $e^{-q(r-r_0)}$ $qr_0 = 3; r_0 = 2.221 \text{ \AA}$	-1.291	0.646	0.0
(d) $e^{-q(r-r_0)}$ $qr_0 = 4; r_0 = 2.221 \text{ \AA}$	-1.460	0.730	0.0
(e) $e^{-q(r-r_0)}$ $qr_0 = 3; r_0 = 2.221 \text{ \AA}$	-1.352	0.578	-0.053
(f) $e^{-q(r-r_0)}$ $qr_0 = 3; r_0 = 2.493 \text{ \AA}$	-0.935	0.400	-0.037

differences are likewise insensitive to the choice of parameters. In our calculations we use $N=4$, which corresponds to including up to four-body potentials. The motivation for this truncation is to obtain a simple r -space physical picture of the rudiments of the structural-energy differences. Quantitative calculations must, of course, go to higher order. We have performed calculations for higher values of N (up to 16), and found that the $N=4$ results typically account for roughly 50–60% of the structural-energy differences. The dominant chemical trends are also obtained at this level.

III. RESULTS

We have considered the energetics of six PTP crystal structures: the $A15$ structure, the $MgCu_2$ Laves-phase structure, the σ -phase structure, the χ -phase structure, the $AlMgZn$ structure, and the Ti_2Ni structure.¹⁶ This collection contains all of the characteristic polyhedra defined by Frank and Kasper.¹⁷ The structural energies are calculated with parameters appropriate for the V-Rh system.¹⁸ This is chosen because it forms the relatively simple $A15$ structure, and its d -electron count and atomic-size ratio are such that it is close to the middle of the $A15$ range obtained in the empirical study of Ref. 6, and may thus be considered to be a “typical” $A15$ system. The structures are treated as fixed atomic volume, which is obtained via Vegard’s law from elemental volumes calculated for the fcc lattice.

Figure 1 shows a decomposition of the structural-energy difference between the PTP structures and the fcc structure into two-, three-, and four-body terms. This decomposition breaks the energy difference down into pair terms coming from μ_2 , μ_4 , and the repulsion energy, three-body terms from μ_3 and μ_4 , and four-body terms

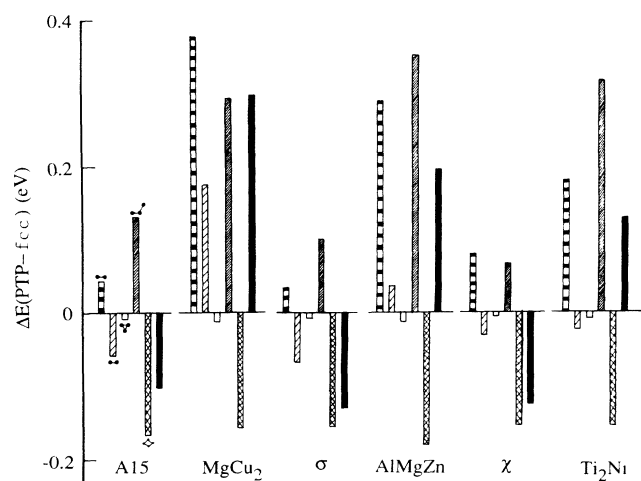


FIG. 1. Decomposition of energy difference between PTP structures and the fcc structure. Histograms show two-moment pair terms (horizontal stripes), four-moment pair terms (sparsely hatched), three-body terms from the third moment (open), three-body terms from the fourth moment (finely hatched), four-body terms (cross-hatched), and total energy difference (solid).

from μ_4 . In addition, the pair terms coming from an analysis based only on μ_2 and the repulsive contribution are shown (horizontal stripes) for each structure. We will call these the atomic-size terms. The $A15$ and $MgCu_2$ structures have the V_3Rh and VRh_2 stoichiometries, respectively; these are compared to the Cu_3Au structure and a combination of the Cu_3Au and $CuAu$ structures on the fcc lattice. The remaining structures are much more complex, and to simplify the interpretation we have simply used atoms with averaged values of the parameters of the constituents; in these cases we compare to the fcc structure.¹⁹ In each of the cases, we see a large stabilizing contribution from the four-body terms, of roughly the same magnitude. In the $A15$ -, σ -, and χ -phase structures the atomic-size terms are fairly small and are dominated by the four-body terms. However, in the $MgCu_2$, $AlMgZn$, and Ti_2Ni structures the difference in size between the sites is so large that the atomic-size terms give a very large destabilizing contribution, which exceeds the electronic four-body terms. This is consistent with the absence of the $MgCu_2$ phase in the V-Rh phase diagram. As shown in Table II, the four-body terms are of comparable magnitude in all the structures that we have examined. The predominance of the four-body terms in the $A15$ -, σ -, and χ -phase structures is consistent with the poor correlation of observed PTP phases with atomic-size ratios, particularly with the above-mentioned “size reversals” in the $A15$ structure.⁶

Our cluster expansion for the total energy allows for a convenient description of the relationship of the geometries of the PTP phases to their associated energies. Its simplest terms, the stability of the PTP phases may be thought of as arising from a competition between atomic-size effects and angular interatomic forces. The four-body angular terms enhance PTP stability. Though we will not describe the three-body terms in detail, we have found that these terms reflect the atomic size in our four-moment picture.¹⁵ The stabilizing effects of the four-body terms can be readily understood by an analysis of the corresponding atomic distribution functions for the six PTP structures treated as well as the fcc structure. Figure 2 shows the numbers of different types of four-body clusters in these structures as functions of the angle θ (the notation for the four-body clusters is defined in the inset of the figure). For simplicity, we consider only those clusters with $\phi < 45^\circ$, since the others make much smaller contributions. The major feature distinguishing all of the PTP structures is the suppression of square clusters with $\theta=90^\circ$. In the completely PTP phases

TABLE II. Four-body contributions ΔE_4 to $\Delta E(PTP-fcc)$.

Structure	ΔE_4 (eV/atom)
$A15$	-0.17
σ phase	-0.16
χ phase	-0.16
$MgCu_2$	-0.16
$AlMgZn$	-0.18
Ti_2Ni	-0.16

(A15, MgCu₂, σ , and AlMgZn), the 90° squares are absent. In the remaining two (χ and Ti₂Ni), their contributions are very small. The four-body potential, plotted below the distribution functions, has a pronounced maximum at $\theta=90^\circ$. Thus all of the PTP structures have a relative stabilizing contribution from this effect. In addition, the average values of θ in the two main groupings

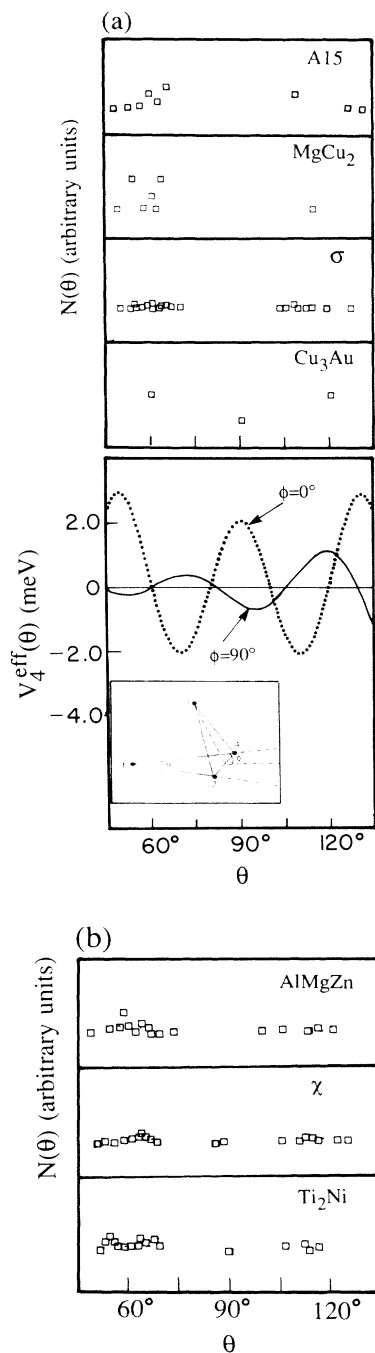


FIG. 2. Four-body potentials and angular histograms. Histograms show number of four-body clusters functions of angle θ for various structures (geometry defined in inset). Shown at bottom of panel (a) are plots of the four-body potential for $\phi=0^\circ$ and 90° .

are shifted in slightly from 60° and 120°, which gives an additional stabilizing contribution. We note that the shape of our V_4^{eff} is similar to that obtained by free-electron theory.²⁰ As mentioned above, the four-body contribution ΔE_4 to the stabilization energy is essentially the same for all of the PTP structures (cf. Table II). This supports the use of topology (tetrahedral versus octahedral packing) as a valid concept in classifying alloy structures.

The strength and magnitude of V_4^{eff} are strongly dependent on the d -electron count N_d of the alloy. This effect arises because of the factor $\partial E/\partial \mu_m$ which is present in Eq. (4). In Fig. 3 we show the band-filling dependence of the prefactors for the two-, three-, and four-body terms. The two-body terms are modulated by a factor which is strongest at half-filling. The four-body terms, on the other hand, are modulated⁸ by an oscillatory function of band filling, and display the most pronounced chemical trends. For nearly-half-filled bands we see that the four-body potentials are modulated by a positive factor, while for nearly empty or filled bands the factor is negative. The result of this oscillatory behavior is that square four-atom clusters disfavor the fcc structure for nearly-half-filled d -bands, while for the nearly-empty-band limit such squares become energetically favorable. V_4^{eff} changes sign and begins to stabilize the fcc structure at $N_d=3.0$ and 7.0. This region of d -electron counts favor-

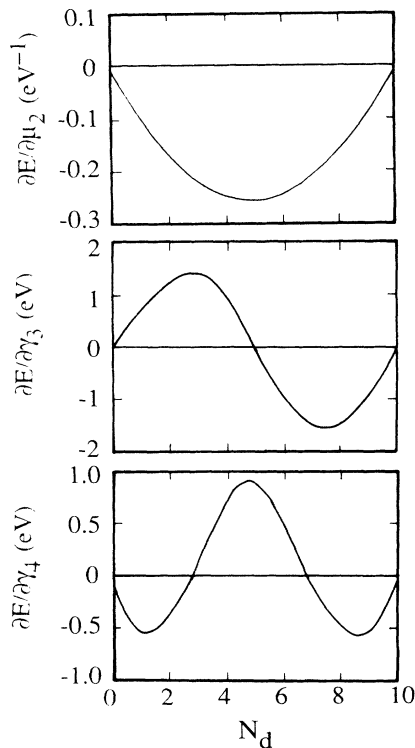


FIG. 3. Prefactors of two- (top panel), three- (middle panel), and four- (bottom panel) body potentials as a function of band filling N_d . Here $\gamma_n = 5^{n/2-1} \mu_n / \mu_2^{n/2}$ is a dimensionless n th moment.

ing the PTP phases corresponds fairly well to the average d -electron counts of 3.0–5.0 that we obtain from the PTP phases tabulated in Ref. 6, assuming 1.5 s - p electrons per atom. At the V_3Rh stoichiometry, the V - Rh system considered here has $N_d = 4.5$ if 1.5 s - p electrons per atom are assumed, and is thus inside the PTP region.

Because of the connection [cf. Eq. (4)] between the effective potentials and the moments, we can describe the stabilizing contribution of the four-body terms in terms

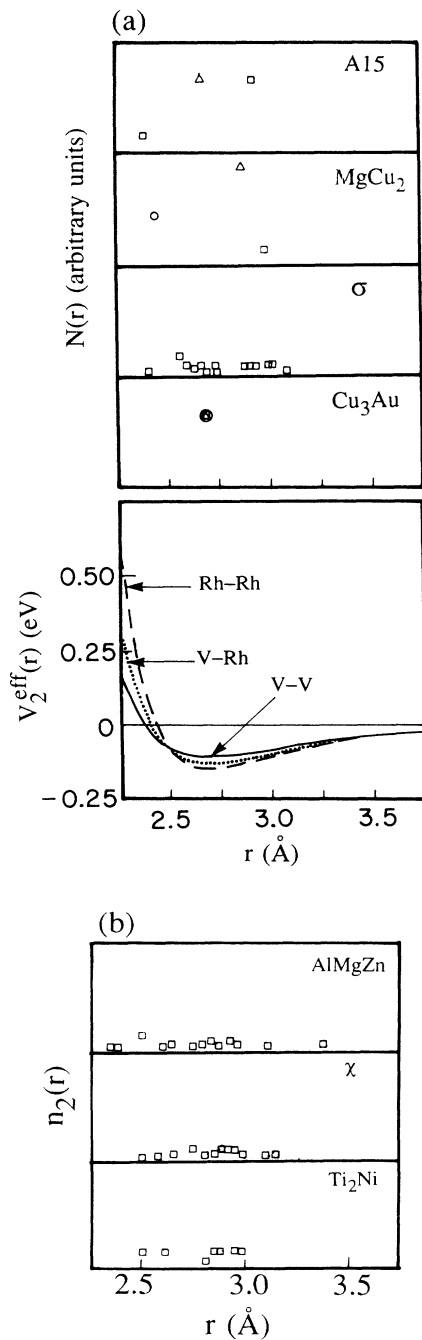


FIG. 4. Two-body potentials derived from μ_2 and repulsive term, together with pair histograms. Histograms show number of near neighbors vs separation distance for various structures.

of the shape of the density of states (DOS). The fourth moment, which the four-body potentials reflect, provides a measure of the weight of the DOS around the band center.²¹ If the fourth moment (scaled by the bandwidth) is small, then the DOS will have a lower value near the band center than for a density of states with a large fourth moment. When the Fermi level falls in this “pseudogap” resulting from the lower μ_4 , the structure will be energetically preferred relative to a structure without a pseudogap.

As mentioned in Sec. II, the angular dependence of the potentials arises from the fact that the Hamiltonian couples d -states. In the context of an s -band Hamiltonian, the three- and four-body terms have no angular dependence. Because the PTP structures have more four-body clusters per atom than in the fcc structure, the four-body contributions in an s -band model would *disfavor* the PTP structures. It is the phase cancellation between contributions from different paths, arising from the angle-dependent couplings, which makes the electronic enhancement of PTP stability possible at all.

An analysis of the atomic-size terms is also revealing. In Fig. 4 we show the distribution of near-neighbor separations for all six of the PTP structures as well as for the fcc structure. We also show the effective pair potentials derived from μ_2 and the repulsive terms. These potentials reflect the atomic-size constraints present in these structures. The atomic sizes of V and Rh are fairly similar, so the minima of the V - V , V - Rh , and Rh - Rh potentials are not far separated. Thus the fcc structure is the most favorable at the pair level, since all nearest-neighbor bonds have the same length, and this length can be adjusted to coincide with the minima of the pair potentials. All of the PTP phases, in contrast, display fluctuations in bond lengths of 20% or more. If the atomic sizes are similar, this provides a destabilizing contribution. If the atomic sizes are distinct, a stabilizing contribution can result. In the Laves phases, this contribution can be as large as 0.3 eV/atom, comparable to the stabilizing four-body terms. However, in the σ , $A15$, and χ phases, even in the most favorable cases the magnitude of the stabilization energy due to the pair terms is less than 0.1 eV per atom, smaller than that of the electronic terms. The distinction between Laves and non-Laves phases is strongly supported by the empirical analysis⁶ of the σ , $A15$, χ , and Laves phases which found a much stronger correlation between atomic size and stability for the Laves phases.

IV. CONCLUSIONS

In summary, we have shown that the dominant interaction favoring transition-metal PTP structures, as a class, over the fcc structure, is a four-body angular interaction whose contribution is roughly independent of the type of PTP structure. The sign and magnitude of the interaction depend strongly on the d -electron count of the alloy. Thus we expect that PTP packing is not universally preferred, even locally, in nonperiodic systems, such as liquids, glasses, and icosahedral phases. To obtain even the correct chemical trends in the structural

energetics of such systems, it will be necessary to include angular forces of the type described here, in addition to the atomic-size effects which have generally been emphasized in atomistic simulations.

The type of analysis carried out in this paper has demonstrated the existence of favorable energetic contributions which are found in all of the PTP structures. We believe that the universal factors favoring local tetrahedral packing in the PTP phases also play a role in determining the types of local coordination polyhedra found in transition-metal quasicrystals. In particular, the Mn constituents of the Ti-Mn quasicrystal should be expected to be components of polyhedra with a paucity of 90° bond angles. According to the previous discussion, this would correspond to a reduced value of the DOS at

the Fermi level. Although this quantity has not been measured for transition-metal quasicrystals, the absence of magnetic moments on the Mn sites²² suggests a reduced DOS at the Fermi level. This is also found in specific-heat measurements²³ for a number of other quasicrystals.

ACKNOWLEDGMENTS

We appreciate useful suggestions and comments from D. Chrzan, M. Daw, C. Henley, J. Holzer, K. Kelton, M. Mills, and D. Pettifor. This work was supported in part by the U.S. Department of Energy under Grant No. DE-FG02-84ER45130.

*Present address: Theoretical Division 8341, Sandia National Laboratories, P.O. Box 969, Livermore, CA 94550.

¹A review of these structures may be found in A. K. Sinha, *Prog. Mater. Sci.* **15**, 79 (1972).

²D. R. Nelson and F. Spaepen, in *Solid State Physics: Advances in Research and Applications*, edited by H. Ehrenreich and D. Turnbull (Academic, New York, 1989), Vol. 42, p. 1.

³C. L. Henley and V. Elser, *Philos. Mag. Lett.* **53**, L59 (1986); *Phys. Rev. Lett.* **55**, 2883 (1985).

⁴L. E. Levine, J. C. Holzer, P. C. Gibbons, and K. F. Kelton, *Bull. Am. Phys. Soc.* **35**, 330 (1990); L. E. Levine, Ph. D. thesis, Washington University, 1990 (unpublished); L. E. Levine, J. C. Holzer, P. C. Gibbons, and K. F. Kelton (unpublished); L. E. Levine, P. C. Gibbons, K. F. Kelton, and J. C. Holzer (unpublished).

⁵See C. T. Sims, in *Superalloys II*, edited by C. T. Sims, N. S. Stoloff, and W. C. Hagel (Wiley, New York, 1987), p. 217.

⁶R. E. Watson and L. H. Bennett, *Acta Metall.* **32**, 477 (1984).

⁷P. Turchi, G. Treglia, and F. Ducastelle, *J. Phys. F* **13**, 2543 (1983).

⁸P. Turchi and F. Ducastelle, in *The Recursion Method and Its Applications*, edited by D. G. Pettifor and D. L. Weaire (Springer, New York, 1985), p. 104.

⁹R. L. Johannes, R. Haydock, and V. Heine, *Phys. Rev. Lett.* **36**, 372 (1976).

¹⁰F. Ducastelle and F. Cyrot-Lackmann, *J. Phys. Chem. Solids* **29**, 1235 (1968); **31**, 1295 (1970).

¹¹See also A. E. Carlsson, in *Solid State Physics: Advances in Research and Applications*, edited by H. Ehrenreich and D. Turnbull (Academic, New York, 1990) Vol. 43, p. 1.

¹²See R. H. Brown and A. E. Carlsson, *Phys. Rev. B* **32**, 6125 (1985), and references therein.

¹³A. E. Carlsson, *Phys. Rev. B* **32**, 4866 (1985).

¹⁴V. L. Moruzzi (private communication). We use an exponential decay law for the pair potential, and the geometric-mean approximation for the parameters entering the potential between unlike atoms.

¹⁵For a more complete discussion, see R. B. Phillips, Ph.D. thesis, Washington University, 1989 (unpublished).

¹⁶The χ phase and the Ti₂Ni structure are actually only partially PTP. The χ phase has a 13-fold site which is not completely tetrahedrally packed. The Ti₂Ni structure includes some octahedra.

¹⁷F. C. Frank and J. S. Kasper, *Acta Crystallogr.* **11**, 184 (1958); **12**, 483 (1959).

¹⁸We have used coupling strengths of -0.935 , 0.400 and -0.037 eV for the σ , π , and δ symmetries, respectively, at the fcc nearest-neighbor distance r_0 . The r dependence is given by $e^{-q(r-r_0)}$, with $qr_0=3$. The parameters A , λ , and r_0 [cf. Eq. (5)] for the repulsive terms are 0.202 eV, 4.984 \AA^{-1} , and 2.701 \AA (V-V); 0.247 eV, 4.207 \AA^{-1} , and 2.694 \AA (V-Rh); and 0.165 eV, 5.906 \AA^{-1} , and 2.709 \AA (Rh-Rh).

¹⁹We have also performed some calculations for these structures with ordered constituents. For appropriate values of the atomic sizes, this leads to a lowering of the atomic-size energy, to be discussed below.

²⁰J. A. Moriarty, *Bull. Am. Phys. Soc.* **34**, 544 (1989), Abstract E 11 5; *Phys. Rev. B* **38**, 3199 (1988); **41**, 1609 (1990).

²¹For a detailed discussion, see R. H. Brown, Ph.D. thesis, Washington University, 1986 (unpublished).

²²E.-K. Jeong, J. C. Holzer, A. E. Carlsson, M. S. Conradi, K. F. Kelton, and P. A. Fedders, *Phys. Rev. B* **41**, 1695 (1990).

²³J. L. Wagner, J. M. Wong, and S. J. Poon, *Phys. Rev. B* **39**, 8091 (1989).